Heat Mass Transfer (2012) 48:1397–1406
DOI 10.1007/s00231-012-0984-z

ORIGINAL

Experimental comparison of the ability of Dalton based and similarity theory correlations to predict water evaporation rate in different convection regimes

Amin Jodat · Mohammad Moghiman · Morteza Anbarsooz

Received: 11 March 2011 / Accepted: 2 February 2012 / Published online: 26 February 2012

Abstract This paper investigates the ability of two widely used evaporation models: Dalton based correlations and similarity theory results by comparing with experimental measurements. A series of experimental investigations are carried out over a wide range of water temperatures and air velocities for $0.01 \leq Gr/Re^2 \leq 100$ in a rectangular heated pool. The results show that for forced convection regime satisfactory results can be achieved by using the modified Dalton correlations, while, due to ripples appear on the water free surface, similarity theory under predicts the evaporation rate. In the free convection regime, Dalton based correlations even with modification are not able to predict acceptable results. For mixed convection regime, although both the similarity theory and Dalton based correlations without modification are not able to predict the mild non-linearity behavior between water evaporation rate and vapor pressure difference, but they obtain relatively satisfactory results. A dimensionless correlation using the experimental data of all convection regimes is proposed to cover different water surface geometries and air flow conditions.

List of symbols

$D_{H_2o,Air}$	Binary mass diffusion coefficient m^2/s
D_h	Hydraulic diameter of rectangular duct (m)
g	Gravitational acceleration m/s^2
g_{m,H_2o}	Mass transfer coefficient
Gr	Mass transfer Grashof number
H	Height of rectangular duct (m)
h_{fg}	Enthalpy of vaporization (J/kg)
k	Thermal conductivity w/mk
L	Length of water pan (m)
$\dot{m}_e$	Evaporation rate of water kg/m^2h
$m_{f\,H_2o}$	The mass fractions of water
Nu	Nusselt number
P	Pressure (Pa)
Pr	Prandtl number
$P_{v,s}$	Saturated vapor pressure at the water surface
$P_{v,\infty}$	Saturated vapor pressure at the ambient air
R^2	Correlation coefficient
Re	Reynolds number
Sc	Schmidt number
Sh	Sherwood number
T	Temperature (K)
T_s	Free surface temperature (K)
t	Time (h)
V	Velocity of air
W	Width of the test chamber
X_{H_2o}	Vapor mole fraction

Greek symbols

ρ	Density kg/m^3
μ	Dynamic viscosity NS/m^2
$\bar{\rho}$	Mean mixture density of air
φ	Relative humidity

Subscripts

g	Moist air property including dry air and water vapor
s	Properties at the surface of the water

A. Jodat (✉)
Department of Mechanical Engineering,
Bojnourd Branch, Islamic Azad University,
Bojnourd, Iran
e-mail: Amin.jodat@yahoo.com

M. Moghiman · M. Anbarsooz
Department of Mechanical Engineering,
Ferdowsi University of Mashhad, Mashhad, Iran
e-mail: mmoghiman@yahoo.com

M. Anbarsooz
e-mail: m.anbarsooz@gmail.com

free Free convection flow regime
forced Forced convection flow regime
mixed Mixed convection flow regime
∞ Average properties at the ambient air
total Sum of free and forced convection component

1 Introduction

Despite numerous applications of water evaporation in many aspects of nature and industrial engineering, there exists no exact expression for the rate of water evaporation [1]. Considerable efforts have been made to correlate water evaporation rate from free water surface and wet surfaces into both still and moving air [2–6]. The most commonly used correlations are: (1) the correlations based on the John Dalton's theory [7] and (2) the correlations based on the analogy between heat and mass transfer [8].

Dalton stated that water evaporation is proportional to the difference in vapor pressure at the surface of the water and in the ambient air and that, the velocity of the wind affects this proportionality. The general form of Dalton's semi-empirical correlation is as follows [7]:

$$\dot{m}_e = (C_1 + C_2 V)(P_{v,s} - \varphi P_{v,\infty})/h_{fg} \quad (1)$$

where $\dot{m}_e$ is the water evaporation rate, $P_{v,s}$ and $P_{v,\infty}$ are the saturated vapor pressure at the free surface and at the ambient conditions, respectively. φ is the relative humidity and h_{fg} is the latent heat of evaporation. C_1 and C_2 are the constants which are determined experimentally [5]. Numerous researchers have expressed their results based on Dalton's description. They have presented the constants C_1 and C_2 in different convection regimes and different experimental setups [3, 4, 9–11]. Obviously, there exist discrepancies between the coefficients presented by these researchers. The discrepancies are mostly originates from the fact that each of the measurements were conducted in a narrow range of convection regime and the fact that the water evaporation rate is not a simple linear function of vapor pressure difference. The nonlinear dependency of evaporation rate ($\dot{m}_e$) on the vapor pressure difference has been considered by many researchers [2, 5, 12–16] and has become the basis of considerable modifications on Dalton's theory. The modified Dalton based correlation accounting for this nonlinearity is as follows:

$$\dot{m}_e = (C_1 + C_2 V)(P_{v,s} - \varphi P_{v,\infty})^n/h_{fg} \quad (2)$$

where n is a constant. Table 1 presents a summary of the various semi-empirical correlations exist in literature.

The other approach to predict the evaporation rate is the well-known analogy theory which is a standard basis for predicting evaporation rate from a free water surface [8, 17]. Analogy theory states that convective heat and mass transfer are completely analogous phenomena under certain conditions [8]. Based on this theory, the convective heat transfer correlations in the form of the Nusselt number can be employed to evaluate the mass transfer rate if the Prandtl number is replaced by the Schmidt number and the Grashof number replaced by the mass transfer Grashof number [17–19].

Despite the extensive studies on development of both Dalton based correlations and the similarity theory, the necessity of an extensive comparison between these two approaches in different convection regimes is evident. The present study of evaporation measurements has been motivated by the need to assess the abilities of Dalton based correlations and the similarity theory results at a

Table 1 Summary of correlations reported in the literature on water evaporation

Reference	Case	n	Proposed correlation
Dalton [7]	Still air	1	$\dot{m}_e = C(P_{v,s} - \varphi P_{v,\infty})$
Carrier [11]	Still and moving air	1	$\dot{m}_e = 3370(95 + 83.7V)(P_{v,s} - \varphi P_{v,\infty})/h_{fg}$
Rowher [10]	Moving air	1	$\dot{m}_e = (0.125 + 0.0755V)\left(\frac{P_{v,s} - \varphi P_{v,\infty}}{1000}\right)$
Al-Shamiri [15]	Moving air	0.654	$\dot{m}_e = (0.12083V^{1.478})\left(\frac{P_{v,s} - \varphi P_{v,\infty}}{1000}\right)^{0.654}$
Tang and Etzion [5]	Moving air	0.82	$\dot{m}_e = 3600(0.2253 + 0.24644V)\frac{(P_{v,s} - \varphi P_{v,\infty})^{0.82}}{h_{fg}}$
Pauken [2]	Moving air	$1.22 - 0.19V + 0.038V^2$	$\dot{m}_e = a\left(\frac{P_{v,s} - \varphi P_{v,\infty}}{1000}\right)^b$ $a = 0.074 + 0.0979V + 0.02491V^2$ $b = 1.22 - 0.19V + 0.038V^2$
Boetler et al. [12]	Moving air	1.22	$\dot{m}_e = 0.074\left(\frac{P_{v,s} - \varphi P_{v,\infty}}{1000}\right)^{1.22}$
Shah [21]	Still air	–	$\dot{m}_e = C\rho_w(\rho_r - \rho_w)^{\frac{1}{3}}(W_r - W_w)$
Paukenet al. [20]	Still air	–	$\dot{m}_e = 0.035(C_s - C_a)^{1.237}$

wide range of convection regimes ($0.01 \leq Gr/Re^2 \leq 100$). Hence, the main aim of this study is to evaluate if the two above mentioned approaches for predicting evaporation rate are equally suited to accurately describe evaporation rate for different convection regimes. If this is not the case, the limitations of the different approaches will be investigated.

The measurements are performed in a heated water pool inside a wind tunnel. The air velocities used in this investigation ranged from 0.05 to 5 m/s and the water temperatures considered were from 20 to 55°C in approximately 2.5°C increments.

2 Mathematical calculations

Dimensional analysis on the evaporation process reveals that the mass transfer conservation equation is analogous to the heat conservation equation [2]. Therefore, if the corresponding boundary conditions are similar, then the solution of these equations will also be similar. The dimensionless governing equations are as follows [17]:

$$\rho^* \frac{DT^*}{Dt} = \frac{1}{Re \times Pr} \nabla^* \cdot (k^* \times \nabla^* T^*) \tag{3}$$

$$\rho^* \frac{DC^*}{Dt} = \frac{1}{Re \times Sc} \nabla^* \cdot (D^* \times \nabla^* C^*) \tag{4}$$

where ρ^*, k^*, D^*, T^* and C^* are the dimensionless density, conductivity, mass diffusivity, temperature and concentration fields, respectively. Pr and Sc are the Prandtl and Schmidt numbers which are defined as [17]:

$$Pr = \frac{v}{\alpha} \tag{5}$$

$$Sc = \frac{v}{D_{H_2o,air}} \tag{6}$$

where v, α and $D_{H_2o,air}$ are the kinematic viscosity, thermal and mass diffusivities, respectively. The dimensionless parameters mentioned in Eqs. 3 and 4 play a significant role in the evaporation of water. The Nusselt and Sherwood numbers which are widely used to evaluate the heat and mass transfer rates can be defined as a function of Reynolds, Prandtl and Schmidt numbers [8]:

$$Nu = \frac{hL}{k} = f(Re, Pr) \tag{7}$$

$$Sh = \frac{g_{m.H_2o} L}{k} = g(Re, Sc) \tag{8}$$

where L is the characteristic length of the evaporation surface, h and $g_{m.H_2o}$ are the heat convection coefficient and the mass transfer coefficient, respectively. In addition, the binary diffusion coefficient can be estimated as follows [8]:

$$D_{H_2o,Air} = 1.87 \times 10^{-10} \left[\frac{T^{2.072}}{P}\right]. \tag{9}$$

In order to calculate the mass transfer coefficient, the analogy between heat and mass transfer results in the following expression [8]:

$$g_{m,H_2o} = \frac{\dot{m}_e}{m_{f\,H_2o,S} - m_{f\,H_2o,\infty}} \tag{10}$$

where $m_{f\,H_2o,\infty}$ and $m_{f\,H_2o,S}$ are the mass fractions of water within the air and in the saturated form, respectively:

$$m_{f\,H_2o,\infty} = \frac{18.02 X_{H_2o,\infty}}{\left[18.02 X_{H_2o,\infty} + 28.96(1 - X_{H_2o,\infty})\right]} \tag{11}$$

$$m_{f\,H_2o,S} = \frac{18.02 X_{H_2o,S}}{\left[18.02 X_{H_2o,S} + 28.96(1 - X_{H_2o,S})\right]} \tag{12}$$

in which X_{H_2o} is the vapor mole fraction as a function of the vapor pressure (P_{H_2o}) and the atmosphere pressure (P_{atm}) as:

$$X_{H_2o} = \frac{P_{H_2o}}{P_{atm}}. \tag{13}$$

In order to evaluate the saturated vapor pressure $(P_{v,s})$ as a function of temperature, the following relation may be used [18]:

$$P_{v,s} = 10^5 \exp\left[65.832 - 8.2Ln(T_s) + 5.717 \times 10^{-3} T_s - \frac{7235.46}{T_s}\right] \tag{14}$$

where T_s is the free surface temperature.

The evaporation rate can be calculated from the Sherwood number using [8]:

$$\dot{m}_e = Sh \frac{\rho D_{H_2o,Air}}{L} (m_{f\,H_2o,S} - m_{f\,H_2o,\infty}). \tag{15}$$

The Sherwood number must be defined for each convection regime. In order to determine which convection regime is more dominant, the following expression may be used:

$$\frac{Gr}{Re^2} = \frac{\text{Natural convection strength}}{\text{Forced convection strength}} \tag{16}$$

where Gr and Re are the Grashof and Reynolds numbers, respectively, which can be expressed as:

$$Gr = \frac{\bar{\rho}_g (\rho_{g,s} - \rho_{g,\infty}) g L^3}{\mu^2} \tag{17}$$

$$Re = \frac{\bar{\rho}_g V L}{\mu} \tag{18}$$

where $\rho_{g,s}$ and $\rho_{g,\infty}$ are the densities of moist air at the surface of water and at the ambient conditions, respectively. V, is the wind velocity, μ is the air viscosity and L is the

characteristic length of the test chamber. The density of the moist air at the free surface is estimated as the sum of the partial densities of vapor ($\rho_{v,s}$) and dry air ($\rho_{a,s}$) as [19]:

$$\rho_{g,s} = \rho_{v,s} + \rho_{a,s}. \tag{19}$$

In addition, the mean mixture of air in the boundary layer ($\bar{\rho}_g$) define as [19]:

$$\bar{\rho}_g = \frac{\rho_{g,s} + \rho_{g,\infty}}{2}. \tag{20}$$

In order to calculate the density of moist air, the perfect gas equation is used.

For the forced convection flow regimes, Gr/Re^2 is much less than one while for the free convection, Gr/Re^2 is much greater than one. In addition, if Gr/Re^2 is almost one, the flow regime is a combination of both natural and forced convection regimes [8].

In the mass transfer analogy the Sherwood number for the free and forced convection turbulent flow regimes is defined as [8]:

$$Sh_{free} = 0.14(Gr\,Sc)^{0.33} \tag{21}$$

$$Sh_{forced} = 0.034\,Sc^{0.33}\,Re^{0.8}. \tag{22}$$

For the mixed convection flow regime the Sherwood number ($Gr/Re^2 \cong 1$) is given by the following nonlinear combination [8]:

$$Sh_{mixed} = Sh_{free}\left[1 + \left(\frac{Sh_{forced}}{Sh_{free}}\right)^a\right]^{\frac{1}{a}} \tag{23}$$

where a is an exponent which can vary in the range of one and two [2].

3 Experimental setup and measurements

A schematic of the test chamber is shown in Fig. 1. The internal dimensions of the test chamber and the pond depth were considered to be 150 × 100 × 100 cm and 25 cm, respectively. In order to reduce the heat loss via conduction, the pond was made up of medium-density fibre-board and the whole test chamber was isolated using the polystyrene panels of 5 cm in thickness. An aluminum foil tape was used within the interior surfaces to reduce the radiative heat loss and prevent water vapor absorption.

Two immersion heaters were installed near the bottom of the pan to elevate the water temperature to the desired conditions. They were low heat flux heaters with 2,500 W of total power each. The heaters were made of nichrome wire encased in poly (tetra-fluoroetylene) spaghetti tubing.

A draw-thru centrifugal fan was used to exhaust the air and to control the wind velocity within the chamber. Draw-thru fans have the advantage of reducing the extent to which turbulence affects the evaporation rate.

The evaporation rate was evaluated based on two methods. First, the flow rate and the difference between the inlet and outlet absolute humidity were used. Second, with the help of a small pan which was connected to the main pond via a siphon tube [20]. The evaporation rate was calculated based on weighing this small pan using a digital scale over a 10 min period of time. The maximum capacity and the resolution of the scale were about 4 kg and 0.01 g, respectively. However, when the evaporation rate was too slow the measurements were recorded on an hourly basis.

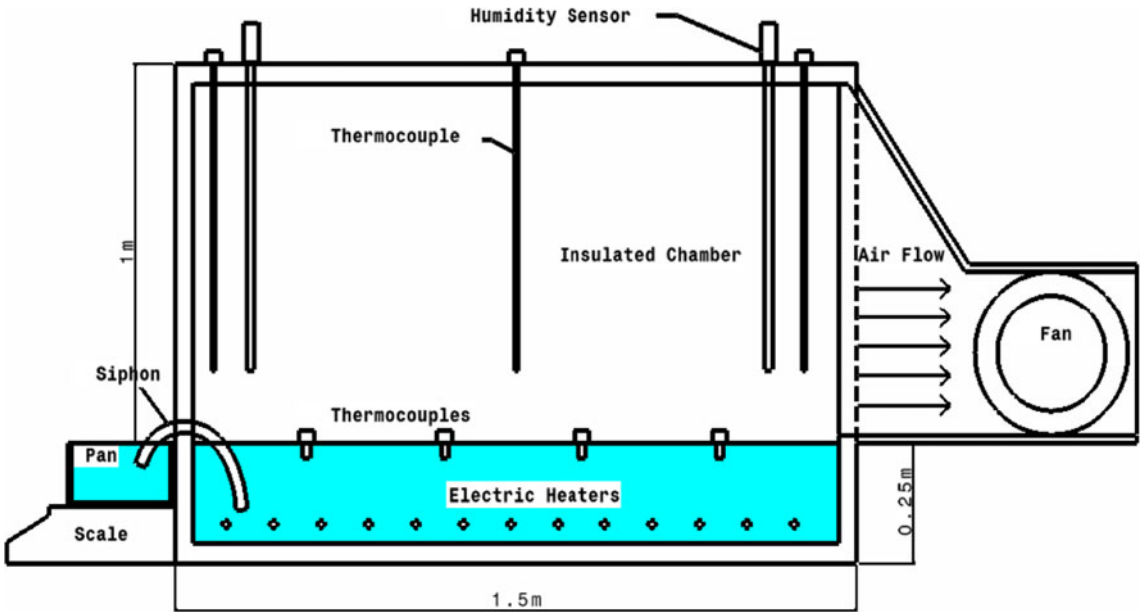

Fig. 1 Experimental test chamber

Table 2 The uncertainty of devices

Device	Uncertainty
Air conditioning system	<1°C
T-type thermocouples	±0.1°C
Humidity transmitter	±1%
Temperature transmitter	±0.1°C
Digital scale	<0.1 (g)
Thermal anemometer	<1%

The mean surface water temperature was measured by averaging the readings of eight T-type thermocouples that were placed 4 cm below the water surface. The pan was divided into eight equal square sections and one thermocouple was placed in the centre of each section.

The water temperatures considered in this investigation ranged from 20 to 55°C in approximately 2.5°C increments. A thermoregulation system was used to guarantee a temperature oscillation of water of about ±0.1°C from the fixed value.

Air relative humidity was measured by two sensors placed at the inlet and outlet of the wind tunnel, 25 cm above the water surface. In addition, the air temperature was measured by a thermocouple located over the midpoint of the evaporation pan.

The air velocity within the chamber was measured using a thermal anemometer, at nine locations across the water surface at about 15 mm above the water surface, and the maximum deviation observed was less than 10%. The average air velocities considered were 0.05, 0.1, 0.3, 0.9, 2, 4 and 5 m/s. The inlet air temperature and relative humidity were controlled using a conventional air conditioning system. A barometer was used to measure the total pressure of the laboratory for each experiment.

The uncertainties of the devices are presented in Table 2. All the measuring instruments were calibrated before the experiments were performed and the data generated by these instruments was captured using a PC data acquisition system.

4 Results and discussion

A wide range of flow regimes namely free, mixed and forced convection ($0.01 \leq Gr/Re^2 \leq 100$) is studied to reveal the abilities of different evaporation correlations. This range of Gr/Re^2 is produced using air average velocities of 0.05, 0.1, 0.3, 0.9, 2, 4 and 5 m/s and the water temperatures from 20 to 55°C. Having produced this range of Gr/Re^2, we have then compared our experimental results with two Dalton based models and the similarity theory results. The Dalton based models used in this study for comparison are those of Rowher [10] and Carrier [11] since they are the most widely used equations based on wind tunnel measurements [2].

Figure 2 shows the effect of vapor pressure difference and air stream velocity on the free water surface evaporation rate. The results presented in this figure cover all free, mixed and forced convection regimes investigated in this study. It can be seen that an increase in the vapor pressure difference/air velocity increases the evaporation rate. The data of this figure have been used to evaluate the capability of widely used evaporation correlations in separate convection regimes.

4.1 Forced convection regime

Figure 3 compares the water evaporation rate results of Dalton based correlations of Carrier [11] and Rowher [10] with experimental measurements of this study for the air velocity of $V = 4$ m/s with the corresponding range of ($0.01 \leq Gr/Re^2 \leq 0.15$). Both Carrier and Rowher have used the conventional Dalton model with the exponent $n = 1$ (in Eq. 2) but with different values for constant coefficients C_1 and C_2. The comparison between the Dalton based correlations with experimental data reveals that the predicted results of correlations strongly depend on C_1 and C_2. The results also show that the Dalton based correlations without modification are not able to predict the non-linear variation of evaporation rate with vapor pressure difference. The experimental results show that the evaporation rate increases nonlinearly with the increase of vapor pressure difference. This occurs because at high evaporation rates (forced convection regime) the vapor density boundary layer is thicker than that expected due to the existence of the surface vapor emission. As the vapor pressure difference increases the surface emission is more intense which slows down the increasing rate of evaporation. According to this behavior, by taking the 1st and 2nd derivatives of Eq. 2 with respect to vapor pressure difference, the following equations could be obtained:

$$\frac{d\dot{m}_e}{d\Delta P} = \frac{1}{h_{fg}} n(C_1 + C_2 V)\Delta P^{n-1} > 0 \tag{24}$$

$$\frac{d^2\dot{m}_e}{d\Delta P^2} = \frac{1}{h_{fg}} n(n-1)(C_1 + C_2 V)\Delta P^{n-2} < 0 \tag{25}$$

hence, it can be concluded that the exponent n must be between zero and one to satisfy the above equations. This is in accord with the experimental data of Marek and Straub [13], Tang and Etzion [5] and Al-Shamimiri [15]. These researchers have suggested that the value of n in Eq. 2 must be <1.

Figure 4 compares the evaporation rate measurements with the results of similarity theory. It can be seen that the

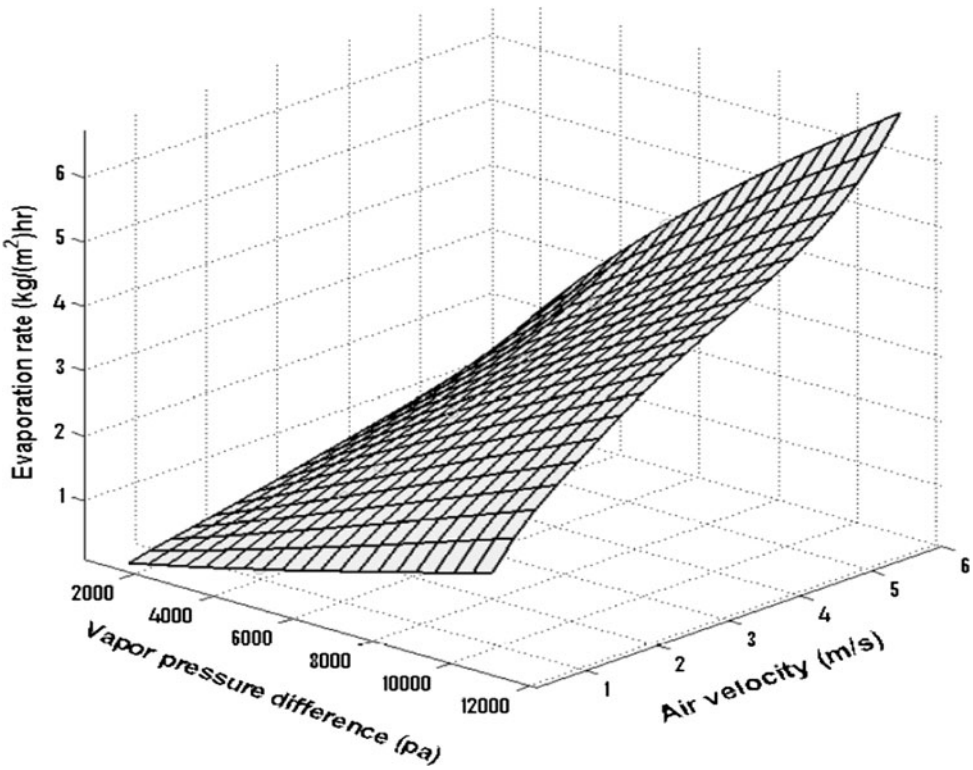

Fig. 2 Effect of vapor pressure difference and air velocity on water surface evaporation rate

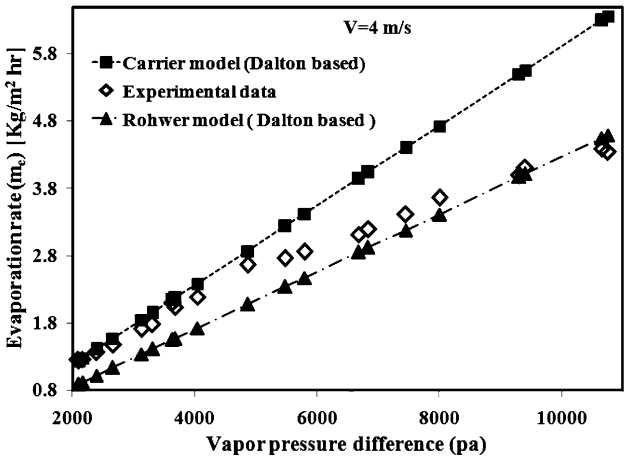

Fig. 3 The comparison between experimental data and Dalton based model results for the forced convection regime ($V = 4$ m/s and $0.01 \leq Gr/Re^2 \leq 0.15$)

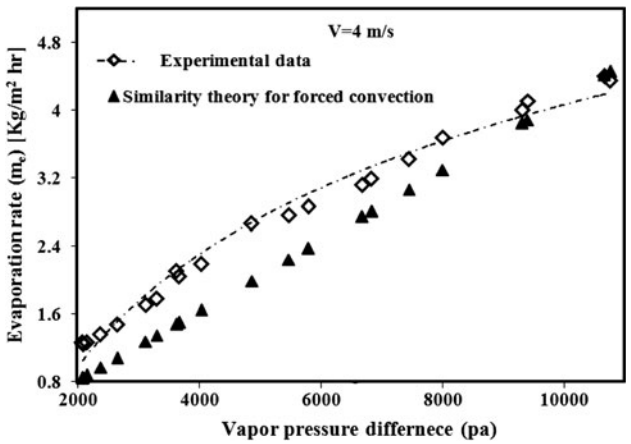

Fig. 4 The comparison between experimental data and similarity theory results for the forced convection regime ($V = 4$ m/s and $0.01 \leq Gr/Re^2 \leq 0.15$)

similarity theory not only is not able to predict the non-linear dependency between water evaporation rate and vapor pressure difference but under predicts the evaporation rate due to the assumptions exist in this theory that some of them are not perfectly true [8]. One of the main assumptions is that the water evaporation surface must be completely smooth, while at high air velocities, ripples appear on the free surface of the water. These ripples act like surface roughness and thus augment the turbulent transport of water vapor [3].

4.2 Mixed convection regime

Figure 5 presents the experimental evaporation rate data as a function of vapor pressure difference in comparison with the Rowher model [10], for the air velocity of $V = 0.9$ m/s with the corresponding range of ($0.3 \leq Gr/Re^2 \leq 3$). It can be seen that, the experimental results in this regime are in good agreement with the Rowher model [10]. The small discrepancy between the experimental data and the Rowher model [7] can be due to the fact that the non-linear

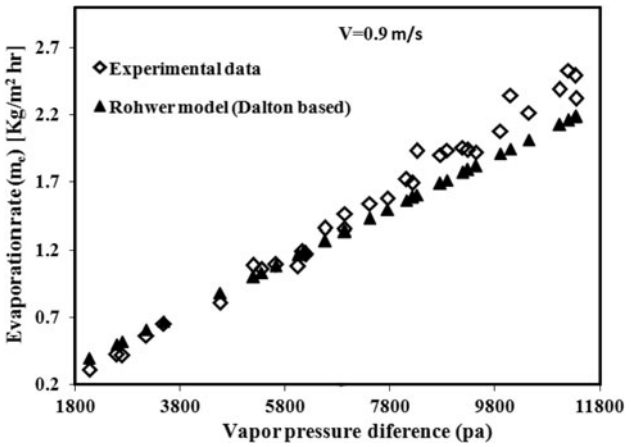

Fig. 5 The experimental data comparison with Dalton based model results for the mixed convection regime ($V = 0.9$ m/s and $0.3 \leq Gr/Re^2 \leq 3$)

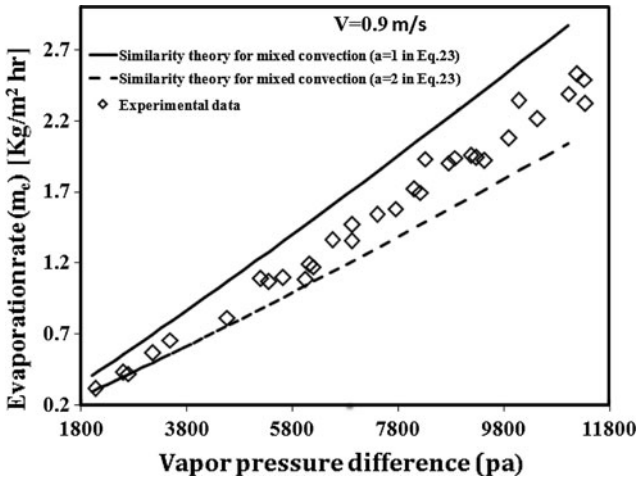

Fig. 6 The comparison between experimental data and similarity theory results for the mixed convection regime ($V = 0.9$ m/s and $0.3 \leq Gr/Re^2 \leq 3$)

dependency of evaporation rate on the vapor pressure difference was not considered in his model (exponent $n = 1$ in Eq. 2). In this convection regime, the experimental results also show that the exponent n in the modified Dalton model (Eq. 2) should be greater than 1 which is in accord with Paukan [2], Moghiman [14] and Boetler [12] results. However, the exponent n can be represented more accurately if it is considered as a function of air velocity. A non-linear regression using SPSS software resulted in the following mathematical model for water evaporation rate

$$\dot{m}_e = 0.001 \times (0.03262V^3 + 0.01814V^2 + 0.04818V + 0.02264)(P_{v,s} - \varphi P_{v,\infty})^{(0.009V^2 - 0.132V + 1.186)}. \quad (26)$$

It must be noted that this correlation is valid for both mixed and forced convection regimes for the cases considered in the present study ($0.01 \leq Gr/Re^2 \leq 25$ and $0.3 \leq V \leq 5$).

The comparison between the similarity theory results [8] and the experimental data are depicted in Fig. 6 for a typical air velocity in the mixed convection regime ($V = 0.9$ m/s). Based on the experimental data in this figure, it appears that the exponent a in Eq. 23 should have a value between 1 and 2 which is also reported previously in the literature [2].

In Fig. 7 the ratio of Sh/Sh_{free} calculated based on the experimental evaporation data are plotted versus the ratio of Sh_{forced}/Sh_{free}. The free and forced convection components of Sherwood number are calculated from Eqs. 21 and 22, respectively. It can be seen that for the ratios of Sh_{forced}/Sh_{free} less than 1.5, the exponent a in Eq. 23 is almost equal to 2.0, while for the ratios of Sh_{forced}/Sh_{free} >1.5, this exponent gradually approaches to 1. Therefore, it can be concluded that this exponent does not have a constant value,

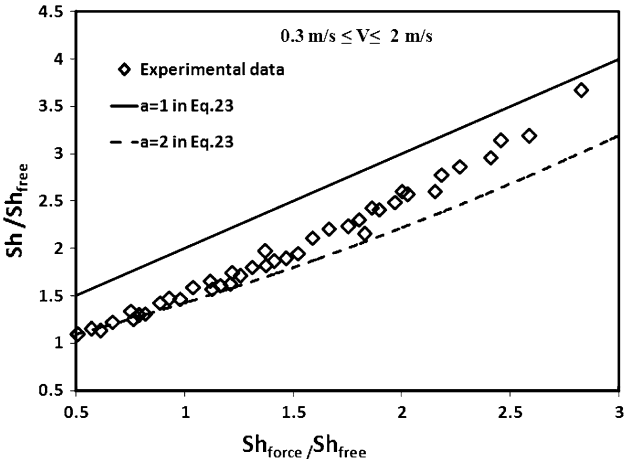

Fig. 7 Dependence of total evaporation rate on the ratio of forced to free convection (comparison between the experimental data and the similarity theory results)

so attention is now paid to find the parameters that the exponent a depends on. Our experimental data reveals that this exponent strongly depends on the air stream velocity while it shows weak dependence on the air temperature and can be neglected. Due to the dominant dependency of the exponent a to the air velocity, the variation of this exponent as a function of air velocity is plotted in Fig. 8. This figure verifies this dependency in a manner that increasing the air velocity decreases the exponent a. The function that best fits our experimental data is a third-order function of air velocity which is as follows:

$$a = -0.6065V^3 + 2.267V^2 - 3.005V + 3.008. \quad (27)$$

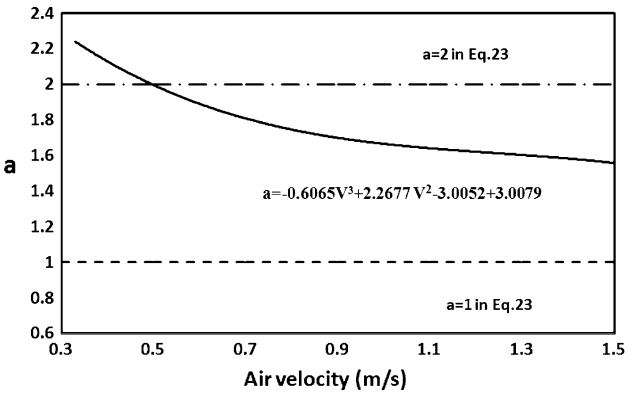

Fig. 8 Variations of the exponent a (in Eq. 23) as a function of air velocity

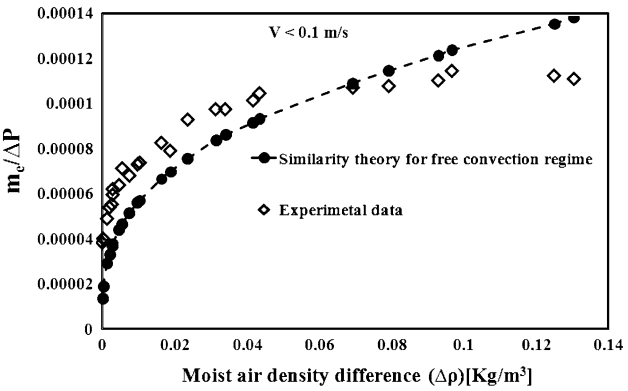

Fig. 10 Comparison of modified evaporation rate ($\dot{m}_e/\Delta P$) for similarity theory and experimental data as a function of density difference in the free convection regime ($V \leq 0.1$ m/s and $Gr/Re^2 \geq 25$)

4.3 Free convection regime

Figure 9 shows the comparison between the measured evaporation data with the results of Rowher's Dalton based model [10] and the results of the similarity theory [8] as a function of vapor pressure difference. The air velocity is less than 0.1 m/s and $Gr/Re^2 \geq 25$. It can be seen that the results of experimental data and similarity theory are close but do not follow a specific trend. The scattering of the results show that the evaporation rate is not a simple function of vapor pressure difference in the free convection regime. In fact, in the free convection regime both the vapor pressure difference and the density difference between the water's surface and the ambient air affect the evaporation rate. This dependency of the evaporation rate on the density difference has also been reported in the literature [20, 21]. Therefore, the Dalton based models which do not take into account the effect of vapor density difference, are not able to satisfactorily predict the results obtained in this convection regime. This can be the reason why the Rowher model predictions are completely far from the experimental data and the similarity theory results.

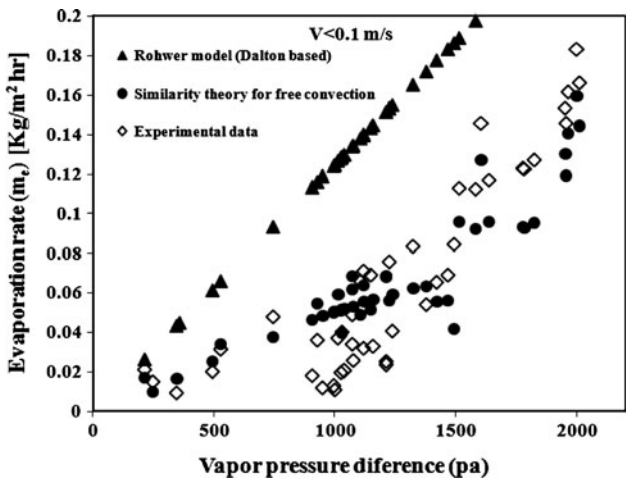

Fig. 9 The comparison between the experimental data, similarity theory and a Dalton based model results for the free convection regime ($V \leq 0.1$ m/s and $Gr/Re^2 \geq 25$)

To take into account the effects of both vapor pressure difference and density difference, in Fig. 10, $\dot{m}_e/\Delta P$ for similarity theory and experimental data are plotted as a function of the density difference. From this figure, it can be seen that $\dot{m}_e/\Delta P$ increases as a power function with increasing density difference. The small discrepancy between the experimental data and the similarity theory is due to the fact that at low density differences the sideways movements of air and stray air currents which are not considered in the similarity theory affect the evaporation rate. These effects have also been observed by Shah [21], Sharpley [22] and Boetler [12]. Their measurements of repeated tests were scattered at low density differences about ±15%.

Considering the vapor density difference effect on the evaporation rate, a new modified Dalton based correlation for free convection regime ($Gr/Re^2 \geq 25$ and $V \leq 0.1$ m/s) is suggested in which the velocity term is substituted with the vapor density difference as follows:

$$\dot{m}_e = 0.01\, C(P_{v,s} - \varphi P_{v,\infty})^n (\rho_{g,s} - \rho_{g,\infty})^{n'}. \quad (28)$$

Performing a non-linear regression on the experimental data of the present work, it is found that the best fit value of the unknown constants to all measurements are $C = 0.069$, $n = 1.105$, $n' = 0.153$. The comparison of the experimental data with the presented correlation is shown in Fig. 11. The good agreement between the experimental data and the proposed model that can be observed in this figure, shows that this modification can make the Dalton based models more applicable in the free convection regime.

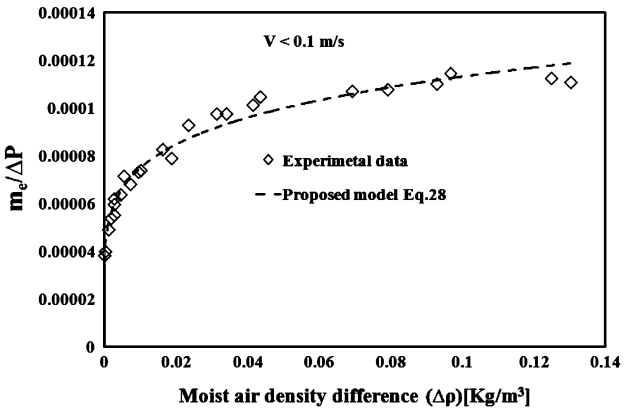

Fig. 11 The modified evaporation rate ($\dot{m}_e/\Delta P$) predicted by the proposed model (Eq. 28) in comparison with the experimental data in the free convection regime ($V \leq 0.1$ m/s and $Gr/Re^2 \geq 25$)

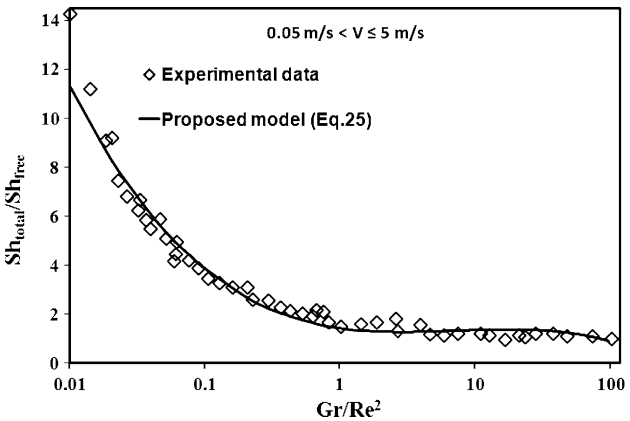

Fig. 12 Variation of the proposed model (Eq. 29) and experimental results with Gr/Re^2 for different convection regimes

In Fig. 12, the variations of the ratio of total Sherwood number to the Sherwood number for the free convection regime Sh_{total}/Sh_{free} versus Gr/Re^2 is plotted. In this figure, the total Sherwood number and the free convection Sherwood number for all data collected in the experiments were calculated using Eqs. 15 and 21, respectively. This figure shows that for $Gr/Re^2 > 10$, the influence of forced convection is almost diminished while for $Gr/Re^2 = 0.1$, the free convection contribution to evaporation rate is about 30% and thus cannot be neglected. The best-fit function from our experimental results is found to have the following form:

$$\frac{Sh_{total}}{Sh_{free}} = 1.441 - 0.345Ln\left(\frac{Gr}{\mathrm{Re}^2}\right) + 0.22\left[Ln\left(\frac{Gr}{\mathrm{Re}^2}\right)\right]^2 - 0.037\left[Ln\left(\frac{Gr}{\mathrm{Re}^2}\right)\right]^3. \quad (29)$$

Equation 29 is valid for a wide range of convection regimes ($0.01 \leq Gr/Re^2 \leq 100$). This dimensionless correlation allows the results of this study to be extended to other evaporation conditions (variation in surface geometry and airflow conditions) rather than those described here.

Table 3 The amount of correlation coefficient (R^2) for Eqs. 26, 28, 29

Equations	R^2
26	0.88
28	0.90
29	0.98

In order to determine the accuracy of the proposed correlations (Eqs. 26, 28, 29), the R square method has been used. The amount of R^2 for these equations has been presented in Table 3.

5 Conclusions

The validity of two different approaches to water evaporation rate calculations, the Dalton based models and the similarity theory results, are assessed by performing experimental measurements in different evaporation regimes. A wide range of Gr/Re^2 ($0.01 \leq Gr/Re^2 \leq 100$) is achieved by applying different air velocities and water temperatures on a heated water pool in a wind tunnel. Based on the presented results, the following conclusions may be drawn:

- In all convection regimes ($0.01 \leq Gr/Re^2 \leq 100$), the accuracy of the Dalton based correlation results strongly depend on C_1 and C_2 constants.
- For forced convection regime, satisfactory results can be achieved by using the modified Dalton correlations, while, due to ripples appear on the water free surface, similarity theory under predicts the evaporation rate.
- For forced and mixed convection regimes, both the similarity theory and Dalton based correlations without modification are not able to predict the non-linearity between water evaporation rate and vapor pressure difference.
- Non-linear data analysis indicates that considering the exponent n in Eq. 2 as a function of wind velocity increases the accuracy of correlation in the mixed and forced convection regimes.
- The ability of the similarity theory to predict the water evaporation rate can be significantly enhanced if we consider the exponent a in Eq. 23 as a function of air velocity.
- In the free convection regime, the similarity theory considers correctly the effects of both vapor pressure difference and vapor density difference, while Dalton

based correlations only take into account the vapor pressure difference.

References

1. Steeman J, Joen C, Belleghem MV, Janssens A, Paepe MD (2009) Evaluation of the different definitions of the convective mass transfer coefficient for water evaporation into air. Int J Heat Mass Transf 52:3757–3766
2. Paukan MT (1999) An experimental investigation of combined turbulent free and forced evaporation. Exp Thermal Fluid Sci 18:334–340
3. Sartori EA (2000) Critical review on equations employed for the calculation of the evaporation rate from free water surfaces. Sol Energy 68:77–89
4. Asdrubali F (2008) A scale model to evaluate water evaporation from indoor swimming pools. Energy Build 41:311–319. doi: 10.1016/j.enbuild.2008.10.001
5. Tang R, Etzion Y (2004) Comparative studies on the water evaporation rate from a free water surface and that from a free surface. Build Environ 39:77–86
6. Moghiman M, Jodat A (2007) Effect of air velocity on water evaporation rate in indoor swimming pools. ISME 8:19–30
7. Dalton J (1802) Experimental essays on the constitution mixed gases; on the force of steam or vapor from water and other liquids in different temperatures, both in a Torricellian vacuum and in air; on evaporation and on the expansion of gases by heat. Mem Manch Lit Philos Soc 5–11:535–602
8. Lienhard JH, Lienhard VJH (2005) A heat transfer text book. Phlogiston Press, New York
9. Ashrae (1999) Ashrae handbook HVAC application. American Society of Heating, Refrigerating and Air-conditioning Engineers, Inc., Atlanta
10. Rowher C (1931) Evaporation from free water surface. US Department of Agriculture in cooperation with Colorado Agricultural Experiment Station. Tech Bull 271:96–101
11. Carrier WH (1918) The temperature of evaporation. ASHVE Trans 24:25–50
12. Boetler LMK, Gordon HS, Griffin JR (1946) Free evaporation into air of water from a free horizontal quiet surface. Ind Eng Chem 38(6):596–600
13. Marek R, Straub J (2001) Analysis of the evaporation coefficient and the condensation coefficient of water. Int J Heat Mass Transf 44:39–53
14. Moghiman M, Jodat A, Javadi M (2007) Experimental investigation of water evaporation in indoor swimming pools. Int J Heat Mass Tech 25(2):43–47
15. Al-Shamimiri M (2002) Evaporation rate as a function of water salinity. Desalination 150:189–203
16. Hinchley JW, Himus GW (1924) Evaporation in currents of air. J Soc Chem Ind 7:57–63
17. Incropera FP, Dewitt DP (2002) Fundamentals of heat and mass transfer. Wiley, New York
18. Boukadida N, Nasrallah SB (2001) Mass and heat transfer during water evaporation in laminar flow inside a rectangular channel—validity of heat and mass transfer analogy. Int J Therm 40:67–81
19. Iskra CR, Simonson CJ (2007) Convective mass transfer coefficient for a hydro dynamically developed airflow in a short rectangular duct. Int J Heat Mass Transf 50(11–12):2376–2393
20. Pauken MT, Tang TD, Jeter SM, Abdel-Khalik SI (1993) A novel method for measuring water evaporation into still air. ASHRAE Trans 99(1):297–300
21. Shah MM (2002) Rate of evaporation from undisturbed water pools to quiet air: evaluation of available correlations. Int J HVAC&R 8:125–131
22. Sharply BF, Boetler LMK (1938) Evaporation of water into quiet air from a one foot diameter surface. Ind Eng Chem 30(10):1125–1131